

Mechanochemical coupling of kinesin studied with the neck linker swing model

Yaogen Shu^{1,*} and Hualin Shi¹

¹*Institute of Theoretical Physics, The Chinese Academy of Sciences, P. O. Box 2735, Beijing 100080, China*
(Dated: March 31, 2022)

We have proposed the neck linker swing model to investigate the mechanism of mechanochemical coupling of kinesin. The Michaelis-Menten-like curve for velocity vs ATP concentration at different loads has been obtained, which is in agreement with experiments. We have predicted that Michaelis constant doesn't increase monotonically and an elastic instability will happen with increasing of applied force.

PACS numbers: 87.16.Nn

I. INTRODUCTION

Kinesin is a molecular motor that transports organelles and membrane-bound vesicles along a microtubule in various cells [1, 2]. It takes hundreds of 8 nm steps (the size of tubulin heterodimers composed of α and β subunits)[3, 4, 5] before detachment and the run length is longer than 1 μm [3, 4, 5, 6]. This is why kinesin is called a processive motor.

Conventional kinesin (hereafter called 'kinesin') is a dimer consisting of two identical $\sim 120\text{kD}$ chains, commonly known as heavy chains. Each heavy chain contains a N-terminal globular head domain, a stalk region which is responsible for heavy chain dimerization, a tether that joins the head and stalk, and a C-terminal fan-shaped tail domain which usually binds cargo for transporting in living cell or bead for applying force in single molecule manipulated experiments [7, 8]. The head domain is a highly conserved region for different members of the kinesin superfamily and contains two binding sites. One binds to microtubule and the other to nucleotides. Two heads alternately hydrolyze one molecular of ATP for each 8 nm step[1, 2, 3, 4, 5, 6, 9, 10, 11, 12, 13]. Sometimes, the 8-nm step can be resolved into fast and slow substeps, each corresponding to a displacement of ~ 4 nm[14]. The tether is a ~ 15 -amino-acid segment. It becomes immobilized and extended towards the forward direction when its head binds microtubule and ATP, and reverts to a more mobile conformation when phosphate is released after ATP hydrolysis[15]. If the tether is replaced by a random sequence of amino acids[16] or if it is cross-linked to nucleotides site[17], the kinesin will lose the capability of stepping. Therefore, the conformational change of tether seems to be necessary for kinesin to step[15].

The motility of kinesin can be explained by a "hand over hand" model[18, 19, 20, 21]. The two heads alternately repeat single- and double-headed binding with microtubule. A simplified binding mode has been proposed[22]. For single-headed binding, the attached head either binds ATP or is empty, whilst the detached

head binds ADP. For double-headed binding, the forward head is empty, whilst the rear head binds either ATP or ADP·P_i.

Kinesin works in a cyclic fashion for several intermediate states. The Michaelis-Menten relation for the rate of ATP hydrolysis is still a basic law[4, 9, 10, 23, 24, 25, 26]. The average stepping velocity, however, also has been experimentally found obeying the Michaelis-Menten law for a range loads[27], which means the mechanochemical coupling is tight, i.e., kinesin hydrolyzes one molecular of ATP for each 8 nm step[12]. With increasing of the applied force, the saturating velocity decreases as expected, however, Michaelis constant surprisingly increases[27]. The role of force in the reaction kinetics can be used to investigate the mechanism of mechanochemical coupling.

In this paper, we present a neck linker swing model to investigate the mechanism of mechanochemical coupling of kinesin. We will discuss the effect of applied force on the reaction kinetics and the elastic instability of the complex composed of neck linker and attached head.

II. NECK LINKER SWING MODEL

When a head attaches microtubule, its tether becomes a rigid rod that can be bent by an applied force, and we call this tether as a neck linker. Otherwise, we call the tether as a flexible chain if its head is detached[15].

An idealized scheme of the relations among nucleotides, microtubule and the tether's conformation is shown in Figure 1a[15, 28, 29, 30]. For attached head, if its catalytic cleft is empty, the neck linker tends to be perpendicular to microtubule. ATP binding will change the catalytic cleft's conformation. The allosteric interaction between two binding sites in the attached head will trigger neck linker to swing to the forward direction[15].

The neck linker swing model consists of two chemical transitions (k_1 and k_3) and two mechanical substeps (k_2 and k_4) as shown in Figure 1b. This model is consistent with the widely accepted model for the kinetic mechanism of kinesin[31]. We just keep their main processes and rearrange them into steps in our model. This approximation is reasonable for the case that ADP concentration is low.

*Electronic address: yaogen@itp.ac.cn

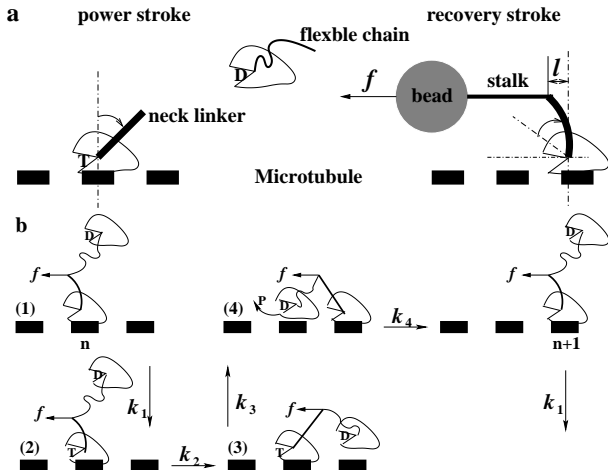


FIG. 1: (a): An idealized scheme of the relations among nucleotides, microtubule and the tether's conformation(not to scale). (b): Neck linker swing model. Two chemical transitions and two mechanical substeps are coupled alternately to each other. T, D and P represents ATP, ADP and P_i respectively.

In this model, the mechanochemical cycle of kinesin includes four steps: ATP binding; power stroke; ADP releasing + ATP hydrolysis and recovery stroke.

A. chemical transition 1: ATP binding

When a head strongly attaches to the microtubule and waits for ATP binding, the neck linker will be bent by the applied force f to the backward direction with displacement ℓ as shown in Figure 1a. The bending energy $E_{\text{bend}} \approx \frac{1}{2}\kappa\ell^2$ and the force $f = dE_{\text{bend}}/d\ell \approx \kappa\ell$ in the case of slight bending, where κ is the bending rigidity.

The attached head will finally bear the bending energy and the energy barrier for ATP binding will increase. So ATP binding rate can be written as:

$$k_1(f) = k_b e^{-E_{\text{bend}}/k_B T} [\text{ATP}] \quad (1)$$

where k_b is ATP binding constant without applied force, k_B is Boltzmann constant, and T is absolute temperature. This relationship holds whether $[\text{ATP}]$ (ATP concentration) is high or low. During attached head is waiting for ATP binding, the free head can't reach any binding site on the track because the end-to-end distance of the flexible chain is not long enough. These sites are separated by a fixed distance ($L = 8 \text{ nm}$) along the rigid microtubule.

B. mechanical substep 1: power stroke

Once the attached head binds an ATP molecule, neck linker will move to the new equilibrium position, and

the free head and bead will be thrown forward. A power stroke occurs. We assume the motion of bead, by which optical tweezer can applies force on motor, is overdamped, the average velocity is

$$\langle \dot{x} \rangle = \frac{1}{\zeta} (\langle f_c \rangle + \langle f_b \rangle - f) \quad (2)$$

where ζ is the viscous coefficient, $\langle f_c \rangle$ and $\langle f_b \rangle$ are average forces generated from ATP binding and releasing of the bending energy respectively, that is, $\langle f_c \rangle + \langle f_b \rangle = (\Delta E_1 + E_{\text{bend}})/(\frac{1}{2}L + \ell)$. The power stroke rate then is

$$k_2(f) = \frac{\langle \dot{x} \rangle}{L/2 + \ell} = \frac{1/\zeta}{L/2 + \ell} \left(\frac{\Delta E_1 + E_{\text{bend}}}{L/2 + \ell} - f \right) \quad (3)$$

ΔE_1 is the energy that power stroke outputs, and originates from the catalytic cleft's conformational change induced by ATP binding[15].

C. chemical transition 2: detached head's ADP releasing and attached head's ATP hydrolysis

With starting of the power stroke, the random motion of the free head will be biased to the forward direction and the flexible chain will be stretched due to neck linker's throwing and the interaction from the nearest β -tubulin monomer, which greatly increases the probability that the free head reaches the next binding site on the track. It first bind weakly, eventually, releases its ADP and attaches strongly to the track. The stretched chain will shrink and transform into a rigid rod, which helps the rear head to split the bound ATP, and one of products, phosphate will be released[15, 22, 30]. This reaction weakens the binding of the rear head with the microtubule and leads it to detach from the track with ADP[15, 22, 30]. We assume the rate of the process from the end of power stroke to the detaching of rear head, k_3 , is independent of applied force.

D. mechanical substep 2: recovery stroke

The tether linked the forward head now becomes the neck linker[15, 22, 30], and will swing to the mechanical equilibrium position. A recovery stroke occurs. Similar with the power stroke, the rate of this step

$$k_4(f) = \frac{1/\zeta}{L/2 - \ell} \left(\frac{\Delta E_2 - E_{\text{bend}}}{L/2 - \ell} - f \right) \quad (4)$$

where ΔE_2 originates from the catalytic cleft's conformational change induced by ADP releasing, which is conformationally the recovery process of ATP binding.

The cycle is now ready to repeat, the difference is that roles of these two partner heads have exchanged. The kinesin dimer has hydrolyzed one ATP and moved forward 8 nm with two substeps[15, 28, 29, 30]. Although there

are more than two chemical transitions as above, all other chemical processes are rapid rate transitions (randomness shows that there are only two to three rate-limiting transitions[27, 32, 33]). We lump all other chemical transitions into k_3 .

III. FITTING AND RESULTS

From the time series shown in Figure1b, the average time to complete a single enzymatic cycle, $\langle\tau\rangle$, can be computed conveniently[33, 34]. The average velocity of kinesin moving along microtubule is

$$v = \frac{L}{\langle\tau\rangle} = L \left(\sum_{i=1}^4 \frac{1}{k_i} \right)^{-1} = \frac{v_{\max}[\text{ATP}]}{K_M + [\text{ATP}]} \quad (5)$$

with

$$v_{\max} = L \left(\frac{1}{k_2} + \frac{1}{k_3} + \frac{1}{k_4} \right)^{-1} \quad (6)$$

$$K_M = \frac{e^{E_{\text{bend}}/k_B T} v_{\max}}{k_b} \quad (7)$$

where v_{\max} and K_M are saturating velocity and Michaelis constant respectively. Obviously, the average velocity obeys the Michaelis-Menten law as observed[27].

In our model, ΔE_1 and ΔE_2 are independent of ATP concentration. We define the efficiency of mechanochemical coupling of kinesin as $\eta = (\Delta E_1 + \Delta E_2)/\Delta\mu$ and assume it is a constant, where $\Delta\mu$ is the free energy excess in one molecule ATP hydrolysis. It must be noted that η defined here is different from the efficiency of motor. We assume kinesin has adjusted ΔE_1 and ΔE_2 to achieve optimal kinetic velocity in evolution. From Eq.(3) and Eq.(4), we yield $\Delta E_1 = \Delta E_2 \equiv \Delta E (< \frac{1}{2}\Delta\mu)$, which is reasonable with the fact that the catalytic cleft's conformational change induced by ADP releasing is conformationally the recovery process of that induced by ATP binding. For simplicity, we introduce the rate of power (or recovery) stroke without load, $k_0 = 4\Delta E/(\zeta L^2)$.

According to Eqs.(3) and (4), the power stroke rate k_2 decreases with increasing of applied force f , whilst the recovery stroke rate k_4 increases as shown in Figure2(d). At a critical applied force, k_2 becomes zero. We call this critical force as stall force. It can be derived as

$$f_{\text{stall}} = \frac{\Delta E + E_{\text{bend}}(f_{\text{stall}})}{L/2 + \ell(f_{\text{stall}})} \quad (8)$$

If applied force is larger than the stall force, the force induced by conformation change can't overcome it to push the kinesin forward along the microtubule.

For the case of slight bending of neck linker, Eq.(8) can be rewritten as $f_{\text{stall}} \approx 2\Delta E/[L(1 + f_{\text{stall}}/(\kappa L))] < \Delta\mu/L \sim 10$ pN with $\Delta\mu \approx 80$ pN·nm under physiological conditions[35], which is in agreement with the experimental data[27]. It must be noted that stall force in

TABLE I: The fitted parameters for experimental v_{\max} and K_M versus f [27] with $k_B T_{\Gamma} = 4.1$ pN·nm

f_{stall} (pN)	κ (pN·nm ⁻¹)	k_b ($\mu\text{M}^{-1}\cdot\text{s}^{-1}$)	k_3 (s ⁻¹)	ζ (pN·s/nm)
6.50	1.88	1.33	120	1.45×10^{-3}

our model is independent of ATP concentration. We can rewrite Eq.(6) and Eq.(7) as

$$\ln \left(\frac{K_M L}{v_{\max}} \right) = -\ln k_b + \frac{1/(2k_B T)}{\kappa} f^2 \quad (9)$$

$$\frac{L}{v_{\max}} = \frac{1}{k_3} + \frac{1}{k_0} \left[\frac{(1 + 2\bar{f})^2}{1 - \bar{f}_{\Delta}(1 + \bar{f})} + \frac{(1 - 2\bar{f})^2}{1 - \bar{f}_{\Delta}(1 - \bar{f})} \right] \quad (10)$$

and use them to fit the measured data of v_{\max} and K_M at different loads[27], where $\bar{f}_{\Delta} = f/[f_{\text{stall}}(1 + f_{\text{stall}}/(\kappa L))]$, and $\bar{f} = f/(\kappa L)$. The fitted values of f_{stall} , κ , k_b , k_3 and ζ are listed in table I, and the two fitted curves, $v_{\max} \sim f$ and $K_M \sim f$, are shown in Figure 2(a).

The fitted stall force $f_{\text{stall}} = 6.5$ pN is consistent with measured value[27]. The total energy outputted in one cycle, $2\Delta E \approx 74$ pN·nm, is less than $\Delta\mu$, which demonstrated again that the fitted values are reasonable. The efficiency of mechanochemical coupling of kinesin, η , is about 93%. However, the efficiency of motor, $f_{\text{stall}}L/\Delta\mu$, is about 65%, which is in agreement with experiments.

It is the motion of a silica bead that is measured in experiment[27]. The radius of the bead, R , is 0.25 μm . The viscosity of water at room temperature, $\tilde{\eta}_w$, is about 0.9×10^{-9} pN·s/nm². The Stokes drag coefficient of the bead can be estimated by $6\pi R\tilde{\eta}_w$, and is about 4.24×10^{-3} pN·s/nm. The fitted viscous coefficient of bead in our model, thus, is comparable with the Stokes drag coefficient for a sphere in 0.5 μm diameter at room temperature.

The widely accepted model for the kinetic mechanism of kinesin[31] has proposed that the ATP binding rate is about 2 $\mu\text{M}^{-1}\cdot\text{s}^{-1}$ and the rate from free head's ADP releasing to attached head's detaching can be estimated about 70 s⁻¹. In our model, ATP dissociating rate k_{-1} isn't taken into account, this is why k_b is slightly less than the proposed value. k_3 also approaches the estimated value.

IV. DISCUSSION

A. K_M no longer increases monotonically with load

Although the recovery stroke will go faster and faster with increasing of applied force, the power stroke will spend more and more time and finally stalls at the stall force, which leads to the concave down of saturating velocity. With low applied force, Michaelis constant will nearly increase exponentially because $e^{E_{\text{bend}}/k_B T}$ increases faster than v_{\max} decreases. With high force,

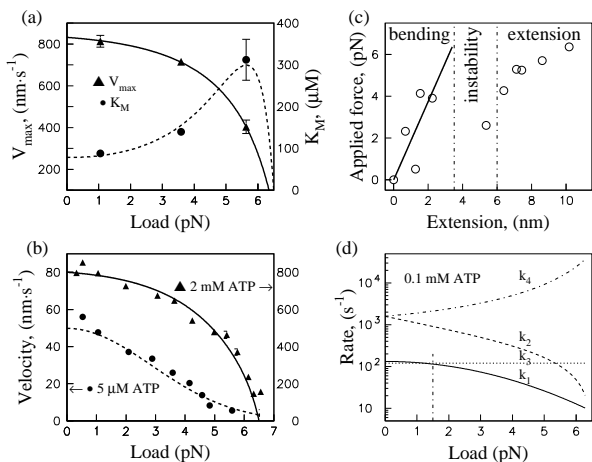


FIG. 2: **(a)**: Fitting to experimental v_{\max} and K_M vs f [27]. The fitted parameters are listed in table I. **(b)**: Dependence of velocity on load at saturated and limiting ATP concentrations. The curves are directly from Eq.(5) analytically with parameters shown in table I, and the experimental data come from Ref[27]. **(c)**: Applied force vs extension. The relation $f = \kappa \ell$ with κ shown in table I is in good agreement with the experimental data[22] at low force. **(d)**: Dependence of rates on applied force at 0.1 mM ATP.

power stroke becomes the rate-limiting step for the single enzymatic cycle, so, K_M will fall fast as v_{\max} shown in Figure 2(a). Michaelis constant no longer increases monotonically with load. The big error bar at high force implies that this prediction is possible.

B. neck linker's bending

Actually, the neck linker's bending has been unconsciously revealed in experiment[22]. With an applied force moving toward the end of microtubule, a simply elastic model can fit all extension of kinesin-microtubule complex for double-headed attaching. But the force-extension relation in Figure 2(c) can't be fitted by a same simply elastic model for all extension for single-headed attaching. With our neck linker swing model, we can image there are three distinctive regions of force. If the force is low, the "Extension" is mainly contributed by neck linker bending. We compare the relation $f = \kappa \ell$ to the experimental force-extension data[22] in Figure 2(c). It is very surprising that our model is in agreement with experiment very well. With the increasing of applied force, a phenomenon of elastic instability[36] will inevitably happen to the complex composed of neck linker and attached head. This is why the extension rapidly increases while the "applied force" falls fast as the measured data in Figure 2(c). After reaching the new mechanical equilibrium, the complex will further extend

with increasing of applied force, and its force-extension relation can be fitted by a simply elastic model again.

C. velocity versus applied force at saturating and limiting ATP concentration

With these reasonable fitted parameters, we can use Eq.(5) directly to compute the dependence of the velocity on load at saturating and limiting ATP concentrations. As shown in Figure 2(b), the theoretical velocity-force relation is in good agreement to experimental data[27]. It is clear that there are three distinctive regimes of applied force: (1) If the load is low, chemical transition 2, the process from free head's ADP releasing to attached head's ATP hydrolysis, k_3 , is the rate-limiting transition at saturating [ATP] and $v \approx Lk_3 \approx 900$ nm/s, which is consistent with what is known about the biochemistry of kinesin[37, 38], while ATP binding is the rate-limiting transition at low [ATP] and $v \approx Lk_1 \approx 50$ nm/s with 5 μ M. (2) If load is high, kinesin will stall at the same force as discussed in section III whether ATP concentration is high or low. (3) If applied force is moderate, the velocity-force curves display different shapes at low and saturating ATP concentration respectively. At very low ATP concentration, the velocity decreases exponentially as k_1 and looks like linear with load because ATP binding is the rate-limiting step. At saturating [ATP], the velocity is concave down with load as discussed in section IV A.

D. two mechanical substeps

The two mechanical substeps in this model are contributed by the two heads respectively. The recovery stroke is always a rapid rate step which corresponds to the observed fast substep[14]. If a moderate load such as 1.5 pN acts on the bead and ATP concentration is maintained at 0.1 mM, the two chemical transitions have the same rate as shown in Figure 2(d). The time spent in ATP binding equals that spent in chemical transition 2. Theoretically, 4.8 nm slow substep and 3.2 nm fast substep can be detected directly by single molecular manipulated techniques such as optical tweezers. The different load-dependence of these substeps' rate may be revealed in the future experiment.

V. CONCLUSION

We proposed the neck linker swing model which divides the single enzymatic cycle into two chemical transitions and two mechanical substeps. Each chemical transition will induce the conformational change in the catalytic cleft and generate a corresponded mechanical stroke. The model can be used to explain the observed substeps[14]. The different load-dependence of these two strokes' rate

may be revealed in the future experiment. We have investigated the mechanism of mechanochemical coupling of kinesin by the influence of applied force on the bending of neck linker. When attached head is waiting for ATP binding, the neck linker is bent by the applied force. The attached head bears the neck linker's bending energy and the energy barrier for ATP binding increases. This is why Michaelis constant increases with applied force. Our theoretical analysis of average velocity of motor in Eq.(5) also obeys Michaelis-Menten law and has been used to fit the observed saturating velocity and Michaelis constant at different loads[27]. The fitted values of chemical reaction rates are in agreement with those in the widely accepted model[31], and the fitted viscous coefficient of bead is also comparable with the Stokes drag coefficient. The stall force is independent of ATP concentration and its fitted value is consistent with the observed data in experiment[27]. The fitted bending rigidity of neck linker can be used to explain the relation of force-extension in

experiment at low force[22]. With these reasonable fitted parameters, we can directly use Eq.(5) to describe the relation between the average velocity and load at different ATP concentrations, which is in good agreement to experimental data[27] as shown in Figure 2(b). In addition, we have predicted Michaelis constant doesn't increase monotonically and an elastic instability will happen to the complex composed of neck linker and attached head with increasing of applied force.

Acknowledgements

We acknowledge useful discussions with Ou-Yang Zhong-can and Ming Li. This work was supported by Special Fund for Theoretical Physics of Postdoctor and National Science Foundation of China.

-
- [1] T.Kreis and R.D.Vale, *Guidebook to the Cytoskeletal and Motor Proteins*, (Oxford Univ. Press, Oxford, ed. 2, 1999) pp.398-402
- [2] N.Hirokawa, *Science*, **279**, 519 (1998)
- [3] S.M.Block, L.S.B.Goldstein and B.J.Schnapp, *Nature*, **348**, 348 (1990)
- [4] K.Svoboda *et al.*, *Nature* **365**, 721 (1993)
- [5] J.Howard, *Annu. Rev. Physiol.* **58**, 703 (1996)
- [6] K.Kawaguchi and S.Ishiwata, *Biochem. Biophys. Res. Commun.* **272**, 895 (2000)
- [7] K.Hirose, L.A.Amos, *Cell. Mol. Life Sci.* **56**, 184(1999)
- [8] N.Hirokawa *et al.*, *Cell* **56**, 867(1989)
- [9] J.Howard, A.J.Hudspeth and R.D.Vale, *Nature* **342**, 154 (1989)
- [10] D.D.Hackney, *Nature* **377**, 448 (1995)
- [11] W.Hua *et al.*, *Nature* **388**, 390 (1997)
- [12] M.J.Schnitzer and S.M.Block, *Nature* **388**, 386 (1997)
- [13] D.L.Coy, M.Wagenbach and J.Howard, *J. Biol. Chem.* **274**, 3667 (1999)
- [14] M.Nishiyama *et al.*, *Nat. Cell Biol.*, **3**, 425 (2001)
- [15] S.Rice *et al.*, *Nature* **402**, 778 (1999)
- [16] R.B.Case *et al.*, *Curr. Biol.*, **10**, 157 (2000)
- [17] M.Tomishige and R.D.Vale, *J. Cell. Biol.* **151**, 1081 (2000)
- [18] K.Kasedal, H.Higuchi and K.Hirose, *Nat. Cell Biol.*, **5**, 1079 (2003)
- [19] C.L.Asbury, A.N.Fehr and S.M.Block, *Science*, **302**, 2130 (2003)
- [20] A.Yildiz *et al.*, *Science*, **303**, 676 (2004)
- [21] W.R.Schief *et al.*, *PNAS*, **101**, 1183 (2004)
- [22] K.Kawaguchi and S.Ishiwata, *Science*, **291**, 667 (2001)
- [23] S.P.Gilbert *et al.*, *Nature*, **373**, 671 (1995)
- [24] S.P.Gilbert, M.L.Moyer, K.A.Johnson, *Biochemistry*, **37**, 792 (1998)
- [25] M.L.Moyer, S.P.Gilbert, K.A.Johnson, *Biochemistry*, **37**, 800 (1998)
- [26] Y.G.Shu and H.L.Shi, *PRE*, **69**, 021912 (2004)
- [27] K.Visscher, M.J.Schnitzer and S.M.Block, *Nature* **400**, 184 (1999)
- [28] R.D.Vale and R.A.Milligan, *Science* **288**, 88 (2000)
- [29] H.Sosa *et al.*, *Nat. Struct. Biol.*, **8**, 540 (2001)
- [30] P.Nelson, *Biological Physics: Energy, Information, Life*, (W.H. Freeman and Co., 2004),pp.441-444.
- [31] R.A.Cross, *TRENDS in Biochemical Sciences*, **29**, 301 (2004)
- [32] S.M.Block *et al.*, *PNAS* **100**, 2351 (2003)
- [33] M.J.Schnitzer and S.M.Block, *Cold Spring Harbor Symposia on Quantitative Biology*, **60**, 793 (1995)
- [34] Sunney Xie, *Single Mol.* **2**, 229 (2001)
- [35] L.Stryer, *Biochemistry*, Fourth Edition (New York: Freeman,1995),pp.443-462.
- [36] L.D.Landau and E.M.Lifshitz, *Theory of Elasticity*, (Peframon Press, 1986), pp.70-84.
- [37] D.D.Hackney, *PNAS*, **85**, 6314 (1988)
- [38] S.P.Gilbert and K.A.Johnson, *Biochemistry*, **33**, 1951 (1994)